Available online at www.sciencedirect.com
SCIENCE DIRECT®
Journal of Applied Geophysics 54 (2003) 247–256
JOURNAL OF APPLIED GEOPHYSICS
www.elsevier.com/locate/jappgeo

Anisotropy in the Earth's crust and uppermost mantle in southeastern Europe obtained from Rayleigh and Love surface waves

Reneta B. Raykova*, Svetlana B. Nikolova

Geophysical Institute of Bulgarian Academy of Sciences, Acad. G. Bonchev str. bl. 3, Sofia 1113, Bulgaria

Abstract

Digital seismograms from 25 earthquakes located in the southeastern part of Europe, recorded by three-component very broadband seismometers at the stations Vitosha (Bulgaria) and Muntele Rosu (Romania), were processed to obtain the dispersion properties of Rayleigh and Love surface waves. Rayleigh and Love group-velocity dispersion curves were obtained by frequency–time analysis (FTAN). The path-averaged shear-wave velocity models were computed from the obtained dispersion curves. The inversion of the dispersion curves was performed using an approach based on the Backus–Gilbert inversion method. Finally, 70 path-averaged velocity models (35 R-models computed from Rayleigh dispersion curves and 35 L-models computed from Love dispersion curves) were obtained for southeastern Europe. For most of the paths, the comparison between each pair of models (R-model and L-models for the same path) shows that for almost all layers the shear-wave velocities in the L-models are higher than in the R-models. The upper sedimentary layers are the only exception. The analysis of both models shows that the depth of the Moho boundary in the L-models is shallower than its depth in the R-models. The existence of an anisotropic layer associated with the Moho boundary at depths of 30–45 km may explain this phenomenon. The anisotropy coefficient was calculated as the relative velocity difference between both R- and L-models at the same depths. The value of this coefficient varies between 0% and 20%. Generally, the anisotropy of the medium caused by the polarization anisotropy is up to 10–12%, so the maximum observed discrepancies between both types of models are also due to the lateral heterogeneity of the shear-wave velocity structure of the crust and the upper mantle in the region.

Keywords: Surface waves; Anisotropy; Earth's crust; Southeastern Europe

1. Introduction

The region of southeastern Europe has a very complex geological structure with many faults, blocks, zones of subduction and collision, and variations in the crustal thickness in a comparatively small area. Usually, only the dispersion of Rayleigh waves was used for obtaining the shear-wave velocity structure and thickness of the crust (Papazachos et al., 1966, 1967; Papazachos, 1969; Rizhikova and Petkov, 1975; Gobarenko et al., 1987; Snieder, 1988; Calcagnile and Panza, 1990; Lomax and Snieder, 1995; Kalogeras and Burton, 1996; Bondar et al., 1995;

* Corresponding author. Tel.: +359-2-9793942; fax: +359-2-9713005.
E-mail addresses: rraikova@server.geophys.bas.bg (R.B. Raykova), sbnik@server.geophys.bas.bg (S.B. Nikolova).

0926-9851/$ - see front matter © 2003 Elsevier B.V. All rights reserved.
doi:10.1016/j.jappgeo.2002.11.001

Zivcic et al., 2000). The thickness of the crust estimated in these studies varies between 25 and 46 km for different parts of southeastern Europe.

To estimate the dispersion curves of Love waves is more difficult, particularly at distances between 500 and 2000 km. This is due to the overlapping of Rayleigh and Love waves at these distances. Nikolova and Yanovskaya (1984) obtained maps of smoothed Rayleigh and Love group velocities at periods 10, 15, 20, 25 and 30 s in southeastern Europe and Asia Minor. Mindevalli and Mitchell (1989) obtained the velocity structure of western and eastern Turkey using single-station measurements of Rayleigh and Love wave group velocities in the period range 8–50 s. They found that the azimuthal variations of these velocities in western Turkey are consistent with the geological information. Yanovskaya et al. (1998) calculated lateral group-velocity distributions for both Rayleigh and Love waves in the period range of 10–20 s in Black Sea and adjoining regions. They inverted local dispersion curves and thus obtained the crust structure along a profile (latitude 43°, longitude between 24° and 42°) down to the depth of 30 km. Recently, Ritzwoller (2000) observed global surface waves within the range of 20–200 s for Rayleigh waves and 20–150 s for Love waves for all of Eurasia. He presented the results of group-velocity tomography for a set of periods for the relative group velocities of Rayleigh and Love waves, computed using models PREM (Dziewonski and Anderson, 1981) and CRUST-5.1/S16B30 (Mooney et al., 1998). The region of study is between 0°N and 85°N and 0°E and 180°E. Many known geological and tectonic structures were observed in the group-velocity maps—sedimentary basins, continental flood basalt, variations in crustal thickness, back-arc spreading, down-going slabs and mountain roots; however, the resolution of the maps is in the range 5.0–7.5°.

During the last decade, many new digital broadband and very broadband stations were deployed in the studied region (southeastern Europe) and at present high-quality digital records of surface waves are available. This enables studies on the Rayleigh and Love surface waves using the method of the frequency–time analysis (FTAN) and allows more precise determination of their dispersion in southeastern Europe. The correct estimation of the dispersion of both types of surface waves gives an appropriate basis to study the transverse anisotropy in the crust and uppermost mantle. In this study, the shear-wave velocity models obtained from the inversion of the dispersion curves of Rayleigh and Love waves were compared and the observed differences in these models were considered as evidence for the existence of transverse anisotropy in the Earth's crust and uppermost mantle in the studied region.

2. FTAN method and floating filtering

Seismic surface waves transport the greatest part of the seismic wave energy; their attenuation is smaller than body wave attenuation and their propagation velocity depends on the wave frequency. Surface waves are the dominating seismic waves on waveform records obtained by long period, broadband and very broadband seismometers at regional and teleseismic distances. From surface wave analysis information about the shear-wave velocity, anisotropy and the attenuation of the medium can be obtained. The greatest problems in data processing and analysis, particularly at local and regional distances, are: the separation of the Rayleigh and Love waveforms; the separation of the fundamental modes from the higher modes and the body waves; off-great-circle propagation caused by inhomogeneities; reflections; and scattering.

One of the most powerful methods for extracting clear surface waveforms and determination of their dispersion curves is FTAN (Dziewonski et al., 1969; Levshin et al., 1972, 1992; Levshin, 1973; Keilis-Borok, 1986). This is an interactive group-velocity-period filtering method, which is designed to identify the dispersion signal and to extract it from noise sources, different wave types (Rayleigh waves or Love waves, overtones and body waves) and scattering coda. FTAN uses multiple narrow-band Gaussian filters and presents the waveform record in a two-dimensional domain: time (group velocity)–frequency (periods). This method enables separation of different wave packages that is possible neither in the time domain nor in the frequency domain. The basic principles of FTAN are presented in detail in Raykova and Nikolova (2000). FTAN uses the floating filtering technique to extract "clear" surface Rayleigh or Love waveforms. The waveform signal

is filtered first by a band pass filter in the frequency domain. Then phase equalisation is applied to the obtained signal and the phase-equalised spectrum is converted by the inverse Fourier transform. A cosine-tapered window is used for filtering the signal in the time domain. The Fourier transform is applied to the transformed signal and the initial phase spectrum is restored. More detail description of floating filtering is given by Raykova and Nikolova (2001).

FTAN and floating filtering can be applied several times for more accurate measurements of the dispersion parameters. Some examples of FTAN diagrams and floating filtering applied to real data are given in Section 4.

3. Data used

Digital seismograms recorded on stations Vitosha VTS (Bulgaria) and Muntele Rosu MLR (Romania) were collected and processed. The seismic station VTS is a part of the MEDNET network (Mediterranean Seismic Network, Roma, Italy). It is equipped with a three-component very broadband seismometer STS-1/VBB and has operated since May 1996. The waveform data are available in SEED and SAC formats from the websites of ORFEUS (http://orfeus.knmi.nl) and IRIS (http://www.iris.washington.edu). Seismic station MLR is a station of the GEOFON network (GeoForschungsNetz, Potsdam, Germany). It is equipped with a three-component STS-2/VBB seismometer and has operated since September 1994. The waveform data were obtained in SEED format from the website of GEOFON (http://www.gfz-potsdam.de). The waveform records of 25 earthquakes, registered on station MLR or on both stations are analysed. The events occurred in the period from January 1997 to December 1999. The magnitude range of the events is 4.8–6.3 mb. The hypocenter parameters of these events were taken from the International Seismological Center ISC (http://www.isc.ak.uk) and National Earthquake Information Center NEIC (http://www.neic.usgs.gov). A map of the events and stations is shown in Fig. 1. Both Rayleigh and Love dispersion curves from 25 events for station MLR and from 10 events for station VTS have been obtained after using the FTAN program.

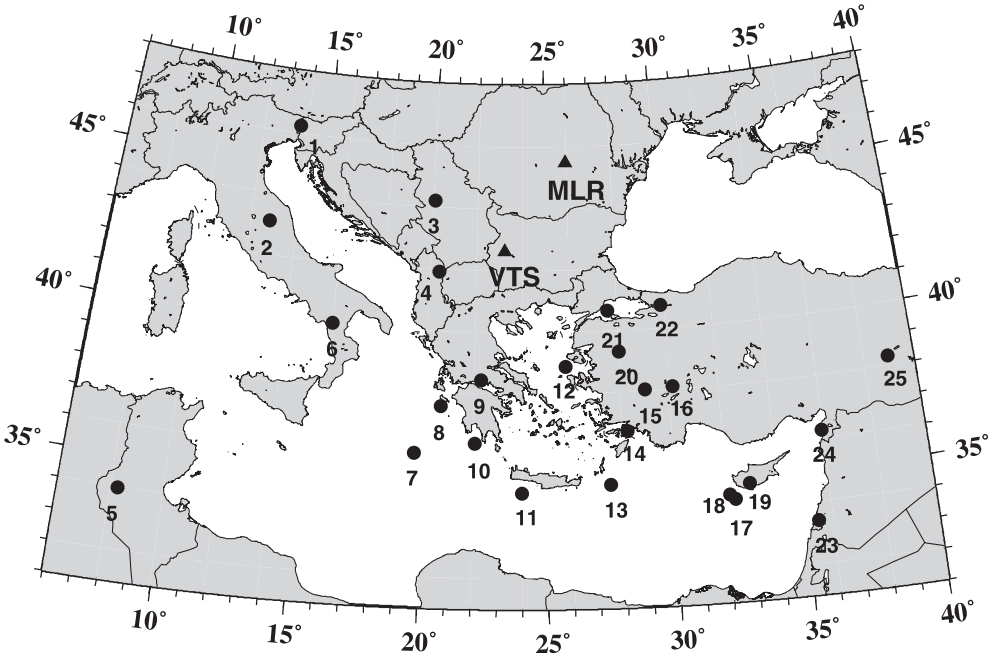

Fig. 1. Map of Balkan Peninsula region and location of the used stations and epicenters of the earthquakes.

4. Data analysis by GFTAN

The FTAN computer package is developed by A. Levshin and his collaborators and is a Colorado University product. The latest GFTAN version is designed for Sun Solaris workstations and is based on the DATASCOPE package for seismic analysis. DATASCOPE is a relational database system, developed by D. Quinlan (IRIS, Washington, USA). The last non-commercial version of the package is DSAP 3.4 and it operates with seismic data in db (extended CSS 3.0) seismic data format.

The two horizontal components (E–W and N–S) of each record are rotated to radial R (along the great-circle path) and transverse T (perpendicular to the great-circle path). Love surface waves are generated by the SH horizontal component of shear waves and should be observed only on the T component. Rayleigh waves are generated by the SV vertical component of shear waves and P compressional waves and should be observed only on R and Z components. This is the case when the surface waves are formed in horizontally layered homogeneous isotropic media. Because of the complex structure of the media, which causes multipathing, reflection and refraction, and because of the anisotropy of the propagating media, for some events Rayleigh waves on the T component and Love waves on the R component and even on the Z component could be observed. This phenomenon has been also observed and studied by Kobayashi and Nakanishi (1998).

The components Z, N, E, R and T were preliminary detrended and filtered by a band pass filter in the range 5–100 s. An example of the FTAN application for event 11 (Crete, 5 November 1997, mb = 5.1, h = 33 km), recorded on station VTS is shown in Fig. 2 for vertical component Z. The FTAN map of the preliminary filtered waveform record is shown in Fig. 2(a). The dispersion curve is defined interactively along the main maximum in the FTAN map. It is the base for floating filtering because it determines the frequency range, the time window, the amplitude and the phase of the derived surface wave. Some examples of the influence of the different dispersion curve

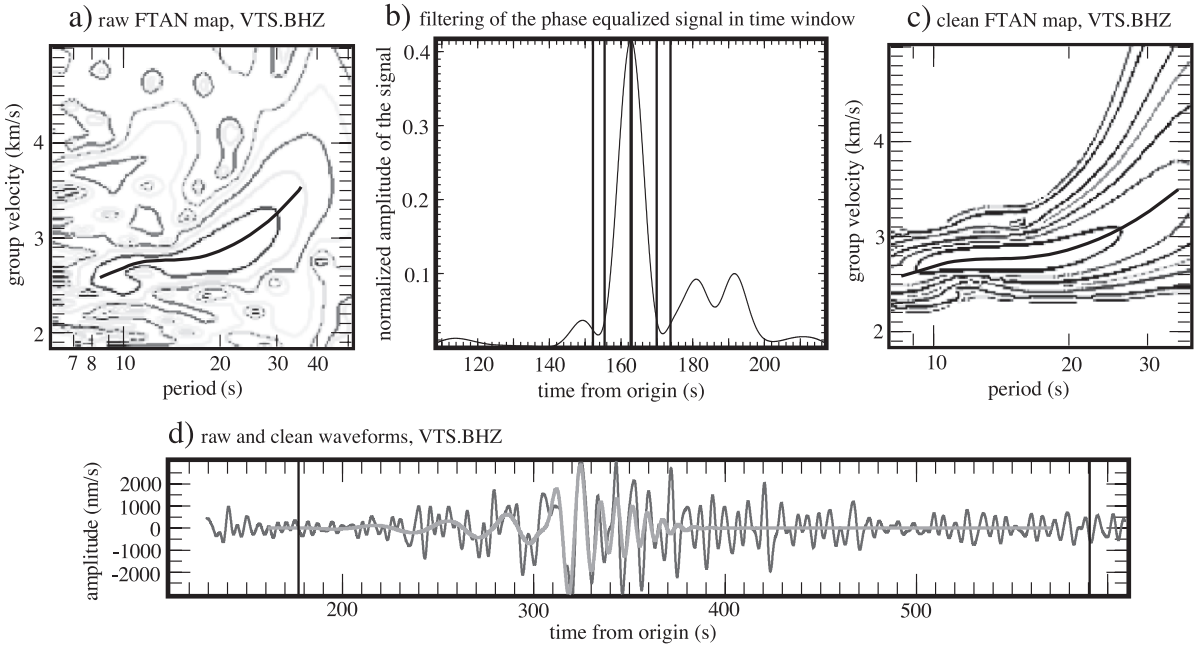

Fig. 2. Analysis of the vertical component Z for event 11 (Crete), recorded at VTS station: (a) the FTAN map of the preliminary filtered waveform and the defined dispersion curve; (b) the compressed phase equalized signal in the time domain with boundaries of cosine-tapered time window; (c) the FTAN map of the cleaned waveform with the corresponding dispersion curve; (d) comparison between "raw" seismogram (thin line) and cleaned Rayleigh waveform (thick line).

positions in the FTAN map can be found in Raykova and Nikolova (2001). The compressed phase equalized signal in the time domain with boundaries of cosine-tapered time window at the step of floating filtering is shown in Fig. 2(b). The FTAN map of the cleaned waveform with the corresponding dispersion curve is shown in Fig. 2(c). Comparison between "raw" seismograms and cleaned Rayleigh and Love waveforms is shown in Fig. 2(d).

Interference of the Rayleigh waves and the Love waves, the high level of the noise and the tracing of the tentative dispersion curve in the FTAN map are the main reasons for wrong surface wave determination in the period range 5–35 s. Relatively short epicentral distances (mainly in the range 500–800 km) do not allow the separation of the waves in time. Preliminary filtered waveforms of Z, E–W and N–S components and waveforms of the Rayleigh wave and the Love wave for event 8 (southern Greece, 18 November, 1997, mb = 5.9, h = 33 km) are shown in Fig. 3. The figure shows clearly that both the Rayleigh wave and the Love wave arrive almost at the same time. The complex structure of the crust (with many nearly vertical boundaries between blocks) and the upper mantle causes surface wave reflections and thus strong polarisation and multipathing has been observed. In some cases strong higher modes, high-frequency interference or some Love waves on the vertical component have been seen on the FTAN diagram. These effects complicate the identification of the dispersion signal on which the measurement method should be applied.

Finally, 70 dispersion curves for Rayleigh and Love fundamental modes were obtained. The observed periods are within the range of 5–50 s and group velocities vary from 2.0 to 4.0 km/s. We observed that generally Love waves are stronger and sharper, and their analysis can be carried out more easily compared to the Rayleigh wave analysis in the studied region.

5. Inversion of the dispersion data

The obtained group-velocity data were inverted by the method proposed by Mitchell and Herrmann (1979) based on Backus–Gilbert inversion theory. The computer implementation of the method is distributed in the shareware package Computer Programs in Seismology (Herrmann, 1992). This interactive

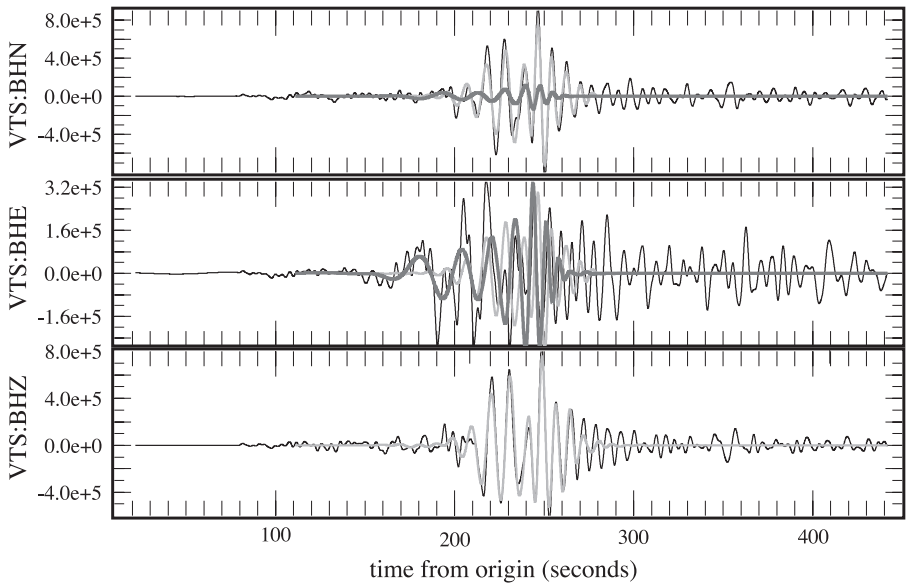

Fig. 3. Overlapped preliminary filtered waveforms of Z, E–W and N–S components (the thinnest black line) of event 8 (south Greece), recorded at VTS station and the Rayleigh wave (thin grey line) and the Love wave (thick dark line).

program inverts dispersion data for plane-layered models and permits both-inversion for velocity and thickness of the layers. We used a differential inversion process, which minimizes both the magnitude of the error vector between observed and computed velocities and differences between adjacent layers, avoiding in this way large velocity changes between adjacent layers.

The starting model is taken from Raykova and Nikolova (2000). It contains 16 layers and a half-space (1 water layer, 7 layers for the crust and 8 layers for the uppermost mantle). The water layer is introduced in the model only if the ray path crosses marine areas. No low-velocity layer (channel) was introduced in the starting model.

Inversion for shear velocity and then inversion for layer thickness was performed at each step. The inversion procedure was stopped when the theoretical dispersion curve fell within the error interval for the observed curve (standard error < 0.1 km/s). The program realization of the inversion allows estimation of weight RMS for the whole calculated dispersion curve in each case. The average value was estimated and used to define the confidence limits of the velocity in the obtained models. The applied method permits obtaining the resolving power-sensitivity of

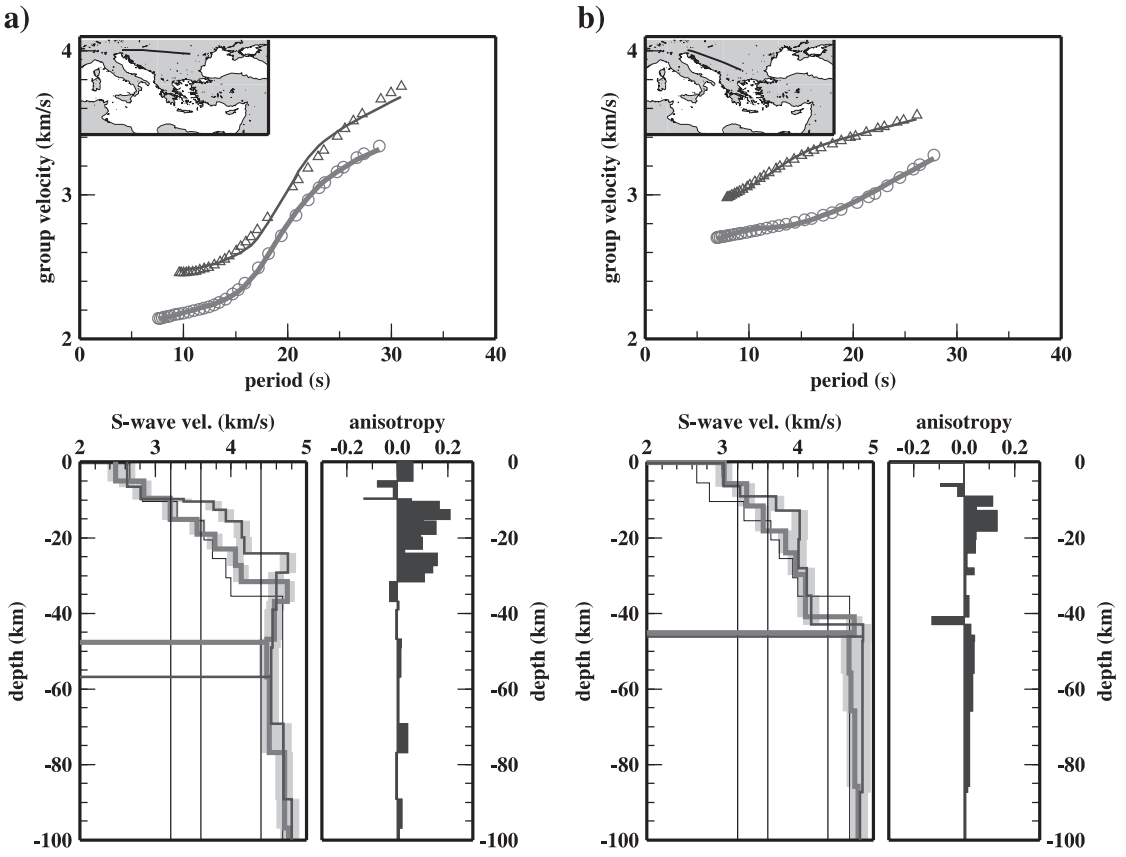

Fig. 4. Results of the inversion of the dispersion curves, event 1: (a) MLR station; (b) VTS station. The dispersion curves for Rayleigh waves (with circles and thick line) and Love waves (with triangles and thin line) are shown on the top graphs in the figure. The circles and triangles show the observed dispersion curves. The solid lines correspond to the dispersion curves after the inversion. The map of the region and the relevant path are shown in the left corner of the top graphs. The bottom graphs represent the models: starting (the thinnest black line), R-model (the thickest grey line) and L-model (thick dark line). The grey regions represent the confidence limits of the models. The horizontal lines (thick for R-model and thin for L-model) specify the depths below which the partial derivatives of the group velocity with respect to the depth exponentially drop. The vertical solid lines defined the boundaries between sediments, upper crust, lower crust and Moho boundary.

the data with respect to the shear velocity or to the thickness of the different layers. The trade-off (regularization) parameter was set so that the model had the best possible resolution with a constraint to be realistic, i.e. large fluctuations of the velocity or thickness were not allowed.

Successful convergence was achieved for all 70 dispersion curves and some results of the inversion are shown in Figs. 4–6. The observed period range of the waves permits reliable definition of shear-wave velocities up to a depth of 100 km, but it was necessary to introduce some layers below this depth in order to avoid a decrease of the shear-wave velocity in the half-space with respect to the shear-wave velocity of the upper layers. The obtained models give an integral shear-wave velocity characteristic of the structure along every wave path (shown on the top graphs in Figs. 4–6).

A comparative analysis between both the R-model and the L-model for each station-epicentre path was performed. We assumed that the shear-wave velocity in the sedimentary layers varies in the range 2.6–3.2 km/s, the velocity range for the upper crust is 3.2–3.6 km/s, velocities between 3.6 and 4.0 km/s are typical for the lower crust, and velocities greater than 4.4 km/s are representative for the mantle (Dachev, 1988; Sollogub et al., 1980). The sedimentary shear-wave velocity is lower (for 23 paths) in the L-models than that in the R-models. For seven paths, velocities in the both models are nearly equal. In only three cases, shear-wave velocity in the L-model is higher than the one in the R-model. The velocities in both of the models are almost equal (in the range 3.0–3.2 km/s) at depths between 8 and 14 km. We considered this depth as a boundary between sediments and upper crust. The thicker sedimentary layers are

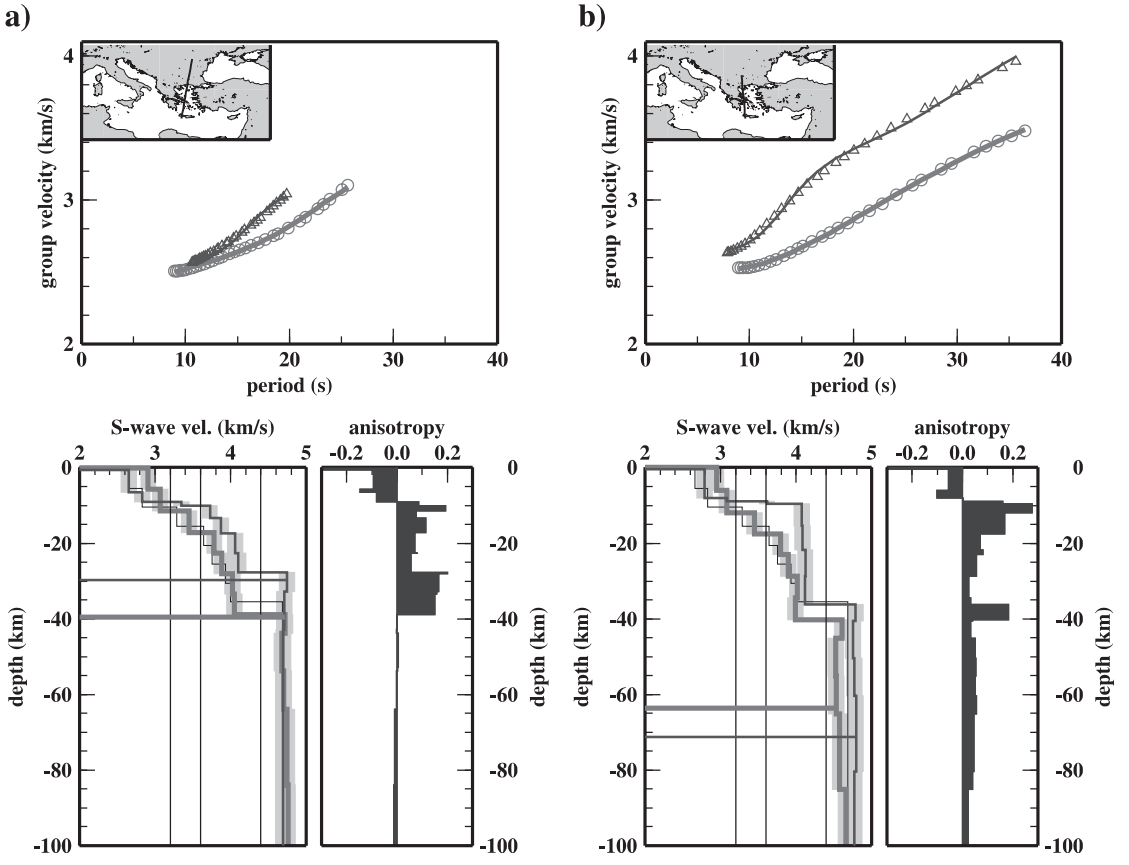

Fig. 5. Results of the inversion of the dispersion curves, event 11: (a) MLR station; (b) VTS station. Symbols used as in Fig. 4.

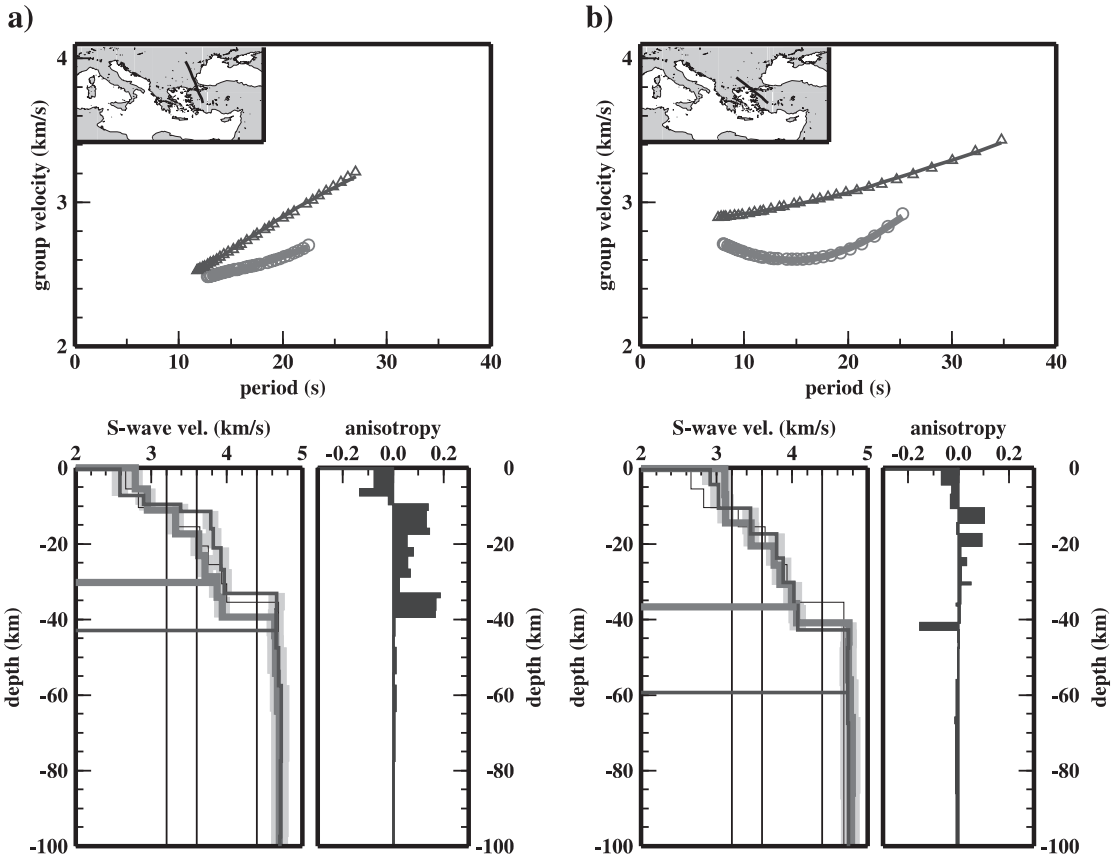

Fig. 6. Results of the inversion of the dispersion curves, event 15: (a) MLR station; (b) VTS station. Symbols used as in Fig. 4.

observed on the models obtained from the records on the MLR station and this result is in agreement with the results of Gobarenko et al. (1987) and Sollogub et al. (1980). The upper crust (layers with shear-wave velocities in the range 3.2–3.6 km/s) has thickness in the range 4–10 km and it is rather thin (2–4 km) in some cases. The thickness of the lower crust is in the range 8–25 km and it is rather different in both, R-models (8–25 km) and L-models (8–18 km). Shear-wave velocity in the L-model is higher than the one in the R-model for 30 paths in the whole crust. Yanovskaya et al. (1998) also found that shear-wave velocities obtained from Love wave data are larger than those from Rayleigh wave data. The Moho boundary is at different depths for both of the models. It reaches depths at about 25–40 km in the L-models and generally it is deeper in the R-models (31–44 km). These results are similar to the Moho boundary depth found in Sollogub et al. (1980).

6. Anisotropy

The differences in the shear-wave velocity models obtained from Love waves and Rayleigh waves may be explained by the existence of transverse anisotropy in the media. The anisotropy coefficient was estimated by the formula (Yanovskaya et al., 1998): $\chi = 2|V_L - V_R|/(V_L + V_R)$, where V_L is the shear-wave velocity in the L-model and V_R is the shear-wave velocity in the R-model. The anisotropy coefficient versus depth is shown on the right bottom graph in Figs. 4–6.

Analysis of the calculated anisotropy coefficient shows that this coefficient has values about 0.08–0.1

for the sedimentary layers, 0.12–0.15 for the crust, and for the layers at depths between 30 and 45 km (around the Moho boundary) the anisotropy coefficient is up to 0.2–0.22. The coefficient of anisotropy sharply decreases below the Moho boundary and it varies between 0.02 and 0.06. The azimuth dependence is observed for the paths to the VTS station at the depths 30–42 km. The coefficient of anisotropy increases in the range 0–0.18 from west to southeast and the difference between the depth of the Moho boundary in the R- and L-models also increases from 0 to 15 km. No similar dependence in the results from station MLR was observed. The anisotropic layers around the Moho boundary for both stations have thickness about 0–10 km. The structure of the crust from Love waves tends to have an abrupt increase and steeper gradient of the velocity beneath the sedimentary layer. However, just above the Moho boundary, the velocities in the L- and R-models are almost equal (for most of the paths $\chi < 0.05$). Thus, the discrepancy in the lower crust seems to decrease compared to the one in the upper crust.

Many authors consider anisotropic Earth's crust and the strongly anisotropic upper mantle from a seismological point of view (Levshin and Ratnikova, 1984; Yanovskaya et al., 1998; Montagner, 2000; Ritzwoller, 2000). Some minerals in the crust and the mantle are anisotropic: the coefficient of anisotropy of the olivine is higher than 0.2, and for the orthopyroxene and clinopyroxene it is 0.1 (Montagner, 2000). But the extremely large values of the coefficient of anisotropy (more than 0.1) could not be due to the anisotropy of the medium (Yanovskaya et al., 1998). Other reason for the extremely large anisotropy can be strongly heterogeneous structure of the studied region. This lateral heterogeneity leads also to Rayleigh–Love discrepancy (Levshin and Ratnikova, 1984; Keilis-Borok, 1986; Yanovskaya et al., 1998). So, probably, both effects, anisotropy of the media and the structure heterogeneity, cause the discrepancies between the L-models and R-models.

7. Conclusions

The application of the FTAN method on digital data from seismic stations VTS and MLR shows encouraging results in the separation of Love and Rayleigh surface waves at regional distances (up to 2500 km). The inversion of dispersion curves for Love and Rayleigh waves based on differential inversion gives steady and reliable results for the structure of the Earth's crust and the uppermost mantle. The boundary between sedimentary layers is well observed in both R- and L-models. The thickness of the sedimentary layer varies within the range of 8–14 km. Discrepancy of R- and L-models is observed for most of the models in the crust. The depth of the Moho boundary is 31–44 km in the R-models and it is 3–15 km shallower in the L-models. This phenomena shows a strong anisotropy related to the Moho boundary where the coefficient of anisotropy reaches a value of 0.2. Both velocity models almost coincide for only 3 ray-paths. Further increasing the amount of data set and regionalization of the dispersion curves are necessary for a detailed study of the anisotropy of the uppermost mantle in southeastern Europe.

Acknowledgements

The authors would like to express their gratitude to Prof. G. Panza and to the colleagues at DST, University of Trieste for the possibility to prepare the paper. Also, the authors wish to thank the referees for their very useful comments and to thank John Douglas for language editing. This research was sponsored by the Bulgarian National Science Foundation under contract MU-903/99.

References

Bondar, I., Bus, Z., Zivcic, M., Costa, G., Levshin, A., 1995. Rayleigh wave group and phase velocity measurements in the Pannonian basin. Seismicity of the Carpatho-Balkan Region 6, 73–86.

Calcagnile, G., Panza, G., 1990. Crustal and upper mantle structure of Mediterranean area derived from surface-wave data. Phys. Earth Planet. Int. 60, 163–168.

Dachev, H.R., 1988. Structure of the Earth's crust in Bulgaria. Technika, Sofia, 334 pp. In Bulgarian.

Dziewonski, A., Anderson, D., 1981. Preliminary reference Earth model. Phys. Earth Planet. Int. 25, 256–297.

Dziewonski, A., Bloch, S., Landisman, M., 1969. A technique for the analysis of transient seismic signals. Bull. Seismol. Soc. Am. 59, 427–444.

Gobarenko, V., Nikolova, S., Yanovskaya, T., 1987. 2-D and 3-D velocity patterns in Southeastern Europe, Asia Minor and the

eastern Mediterranean from seismological data. Geophys. J. R. Astron. Soc. 90, 473–484.

Herrmann, R.B., 1992. Manual for Computer Programs in Earthquake Seismology. St. Louis University, Missouri.

Kalogeras, I., Burton, P., 1996. Shear-wave velocity models from Rayleigh-wave dispersion in the broader Aegean area. Geophys. J. Int. 125, 679–695.

Keilis-Borok, V. (Ed.), 1986. Surface Seismic Waves in Laterally Inhomogeneous Earth. Nauka, Moscow, 277 pp. In Russian.

Kobayashi, R., Nakanishi, I., 1998. Location of Love-to-Rayleigh conversion due to lateral heterogeneity or azimuthal anisotropy in the upper mantle. Geophys. Res. Lett. 25, 1067–1070.

Levshin, A., 1973. Surface and Channel Seismic Waves. Nauka, Moscow, 176 pp. In Russian.

Levshin, A., Ratnikova, L., 1984. Apparent anisotropy in inhomogeneous media. Geophys. J. R. Astron. Soc. 76, 65–69.

Levshin, A., Pisarenko, V., Pogrebinsky, G., 1972. On a frequency-time analysis of oscillations. Ann. Geophys. 28, 211–218.

Levshin, A., Ratnikova, L., Berger, J., 1992. Peculiarities of surface-wave propagation across central Eurasia. Bull. Seismol. Soc. Am. 82, 2464–2493.

Lomax, A., Snieder, R., 1995. The contrast in upper mantle shear-wave velocity between the East European Platform and tectonic Europe obtained with generic algorithm inversion of Rayleigh-wave group dispersion. Geophys. J. Int. 123, 169–182.

Mindevalli, O., Mitchell, B., 1989. Crustal structure and possible anisotropy in Turkey from seismic surface wave dispersion. Geophys. J. Int. 98, 93–106.

Mitchell, B.J., Herrmann, R.B., 1979. Shear velocity structure in the eastern United States from the inversion of surface-wave group and phase velocities. Bull. Seismol. Soc. Am. 69, 1133–1148.

Montagner, J.-P., 2000. Upper mantle anisotropy tomography. 5th Workshop on Three-Dimensional Modelling of Seismic Waves, Trieste, Italy, 38 pp.

Mooney, W., Laske, G., Masters, T., 1998. CRUST 5.1: a global crustal model at $5^\circ \times 5^\circ$. J. Geophys. Res. 103, 727–747.

Nikolova, S., Yanovskaya, T., 1984. Distribution of group velocities of the surface waves of Rayleigh and Love in southeastern Europe and Asia Minor. Bulg. Geophys. J. 10, 83–93. In Russian.

Papazachos, B.C., 1969. Phase velocities of Rayleigh waves in Southeastern Europe and Eastern Mediterranean Sea. Pure Appl. Geophys. 75, 47–55.

Papazachos, B.C., Comninakis, P., Drakopoulos, J., 1966. Preliminary results of an investigation of crustal structure in Southeastern Europe. Bull. Seismol. Soc. Am. 56, 1168–1241.

Papazachos, B.C., Palatou, M., Mindalos, N., 1967. Dispersion of the surface waves recorded in Athens. Pure Appl. Geophys. 67, 95–106.

Raykova, R., Nikolova, S., 2000. Shear wave velocity models of the Earth's crust and uppermost mantle from the Rayleigh waves in Balkan Peninsula and adjacent areas. Bulg. Geophys. J. 26, 11–27.

Raykova, R., Nikolova, S., 2001. Anisotropy in the Earth's crust and uppermost mantle in the Balkan Peninsula and adjacent regions obtained from Rayleigh and Love surface waves. Bulg. Geophys. J. 27, 3–20.

Ritzwoller, M., 2000. Introductory lectures in surface wave seismology. 5th Workshop on Three-Dimensional Modelling of Seismic Waves, Trieste, Italy, 186 pp.

Rizhikova, S., Petkov, I., 1975. Group velocity dispersion and the Black Sea crust structure. Verrof. Zentr. Inst. Phys. Erde. 31, 383–390.

Snieder, R., 1988. Large scale waveform inversion of surface waves for lateral heterogeneity: 2. Application to surface waves in Europe and the Mediterranean. J. Geophys. Res. 93, 12067–12080.

Sollogub, V., Guterh, A., Prosen, D. (Eds.), 1980. The Structure of the Earth's Crust in Central and Eastern Europe From Geophysical Investigations Data. Naukova Dumka, Kiev, 168 pp. In Russian.

Yanovskaya, T., Kazima, E., Antonova, L., 1998. Structure of the crust in the Black Sea and adjoining region. J. Seismol. 2, 303–316.

Zivcic, M., Bondar, I., Panza, G., 2000. Upper crustal velocity structure in Slovenia from Rayleigh wave dispersion. Pure Appl. Geophys. 157, 131–146.